CEAS Aeronautical Journal manuscript No.
(will be inserted by the editor)

Aircraft Noise Generation and Assessment
Novel Liner Concepts

F. Bake · K. Knobloch

July 26th, 2017

Abstract Modern, low emission aero-engine concepts like for instance Ultra-High-Bypass-Ratio (UHBR) designs claim higher demands on the damping performance of acoustic wall treatment, called liner, installed in the engine. New liner concepts are needed providing a more broadband damping efficiency ranging explicitly to the low frequency range. However, space and weight constrains are still also one of the crucial criteria which need to be fulfilled by the liner structure. To overcome this challenge two novel liner concepts are presented here. One concept, the hybrid ZML, combines the classical Single-Degree-Of-Freedom (SDOF) liner with a Zero-Massflow-Liner (ZML) principle. The other one, the FlexiS concept, takes advantage of the intrinsic material damping of flexible walls within the liner structure. A proof of concepts study of both novel concepts is provided highlighting the enhanced damping performance with respect to broadband capacity and low frequency damping.

Keywords aeroacoustics · acoustic damping · liner · wall treatment · novel liner concepts

Introduction

A very significant element for the reduction of aero-engine noise is the application of acoustic wall-treatment, also called liner. The goal is to diminish the engine generated noise on its propagation way out through the inlet and the outlet of the engine. The basic idea of liner relies on the conversion of acoustic energy to other types like flow turbulence or thermal energy. Conventional aircraft liner concepts are based upon a combination of resonance related and viscosity associated dissipation characteristics (see also [23]). The liner consist – like shown in figure 1 – in the classical way of a cavity structure (e.g. honeycomb like), a solid back plate and a facesheet (e.g. perforated plate or wire mesh) facing the target sound field to be damped. Hereby, the resonances of this liner system are either acoustic cavity resonances (e.g. quarter wavelength resonances) or mass-spring-like resonances (e.g. Helmholtz resonances). These conventional liner, also called Single-Degree-of-Freedom (SDOF) liner, provide a damping characteristic in a rather narrow frequency band addressing generally tonal noise sources.

However, the development of modern low emission aero-engines changes the requirements on acoustic liners. New aero-engine architectures like Ultra-High-Bypass-Ratio (UHBR) concepts

Friedrich Bake
Institute of Propulsion Technology, Department of Engine Acoustics, German Aerospace Center (DLR), Germany
E-mail: friedrich.bake@dlr.de

Karsten Knobloch

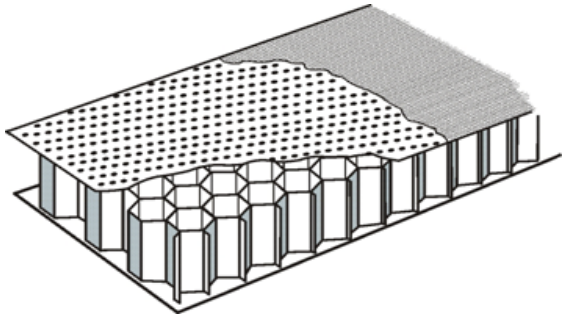

Fig. 1 Conventional liner configuration consisting of a cavity structure (e.g. honeycomb like), a solid back plate and a facesheet (e.g. perforated plate or wire mesh). These liner are also called Single-Degree-of-Freedom (SDOF) liner.

with highly three-dimensional shaped fan blades are acoustically characterized by two main features: 1. The noise signature of these engines exhibits a significant reduction of jet noise and tonal fan noise that goes along with a relative increase of turbomachinery broadband noise sources over large portions of the audible frequency range and 2. the – relatively to the diameter – shortened nacelle structure of the new engine concepts allows only a limited space for liner installation along the propagation path of the generated engine noise. In order to overcome these challenges new liner concepts addressing a broadband frequency range with an improved damping efficiency are needed.

There are already several concepts which adapt the described basic structure in order to improve damping efficiency and effective frequency range. They rely mainly on adding one or more additional degrees of freedom to the resonator structure, e.g. by sub-dividing the basic cells with acoustically effective septa[1],[2]. The same principle is applied in double-degree-of-freedom liners which consist of two honeycomb structures – one atop of the other with a septum in between [7]. Recent developments try to address a larger frequency range by combining cells of different volumes in one single structure [11,12]. By placing larger and smaller cells next to each other and folding the cavities for the larger cells, the effective damping range can be increased with only moderate increase in overall liner-depth [10,25]. A virtual increase of cell depth is also used in the special acoustic absorber concept aiming to address multiple frequencies with a special emphasis on the low-frequency region [19].

The current article introduces two different liner concepts for an enhanced damping performance aiming on the noise reduction requirements of future aero-engine generations. The first part describes a so called hybrid Zero Massflow Liner (hybrid ZML) and the second part presents a novel liner concept with intentionally forced acoustic-structure interaction at the cavity walls (FlexiS – Flexible Structure). The main difference of these two new concepts compared to the liner systems mentioned in the previous paragraph is the introduction of additional damping mechanisms besides the utilization of a multi-degree-of-freedom system.

In the following section of the paper (section 1) the experimental setup with the test facility (1.1) and the measurement procedure (1.2) are explained. In section 2 the study on the first novel liner concept (hybrid Zero Massflow Liner) is presented with the different configurations (2.1) and the results of the corresponding parameter study (2.2). The third section of this paper

Institute of Propulsion Technology, Department of Engine Acoustics, German Aerospace Center (DLR), Germany
E-mail: karsten.knobloch@dlr.de

[1] Ayle, E. (2009). U.S. Patent No. 7,510,052. Washington, DC: U.S. Patent and Trademark Office

[2] http://www.hexcel.com/user_area/content_media/raw/AcoustiCap_brochure_2015.pdf

addresses the second novel liner concept (FlexiS – Flexible Structure) introducing the investigated liner configurations (section 3.1) and describing the experimental results (section 3.2). The paper closes in section 4 with a summary and some conclusions.

1 Experimental Setup

1.1 DUCT-R test rig

The measurements of the current work were performed at the liner flow duct facility of the German Aerospace Center (DLR) in Berlin. This facility, called DUct aCoustic Test rig - Rectangular cross section (DUCT-R), is used for testing sound attenuating duct insets under flow conditions. The rig has a cross section of 60 mm x 80 mm, a length of about 8 m and consists of two symmetrical parts, which are mounted upstream and downstream of the measurement section (see Figure 2). The measurement section provides optionally optical access through glass windows on three sides and supports liners with a length up to 600 mm, which can be mounted at the bottom side. A radial compressor is connected to the upstream part of the duct via a tube system to provide a grazing flow. A maximum Mach number of about 0.3 can be achieved at the duct centerline. The duct provides an overall number of 106 microphone positions which are spread over the rig as described by Busse-Gerstengarbe et al. [4].

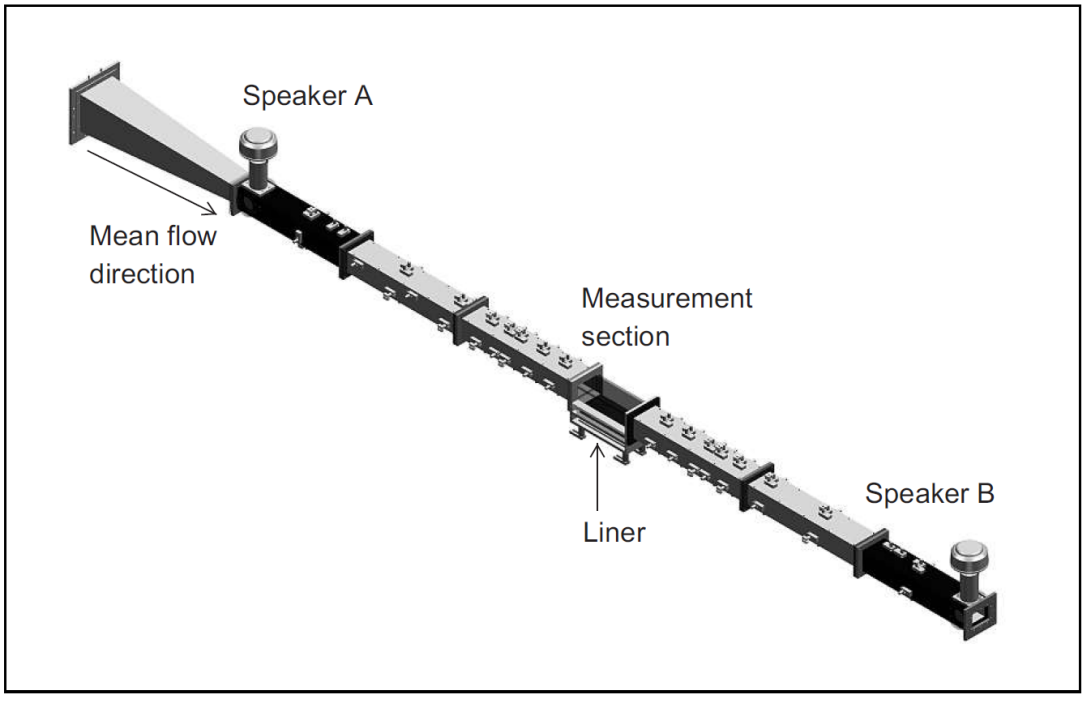

Fig. 2 Principle setup of the DLR liner flow facility DUCT-R

The microphone measurements presented in this work were performed by means of 12 axially distributed G.R.A.S. 40BP-S1 condenser pressure transducers with 26AC pre-amplifiers, which were flush-mounted at the top wall of the duct and distributed symmetrically in the upstream

and downstream section. No circumferential transducer positions were required, since only plane waves were excited yielding a maximum acoustic-excitation frequency of 2160 Hz. Both duct sections were subsequently acoustically excited by a Monacor KU-516 horn driver. The loudspeakers were fed by an Agilent frequency generator, whose signal was amplified with a Dynacord L300 amplifier. Microphone and frequency generator signals were recorded by means of an OROS OR36 data acquisition system for a duration of 20 s with a sampling frequency of 8192 Hz. Additionally, temperature probes were placed downstream of the liner in order to measure the flow temperature and to subsequently determine the speed of sound.

1.2 Measurement Procedure

The damping performance of the liner is evaluated using the dissipation coefficient. This is an integral value of the acoustic energy that is absorbed while a sound wave is passing the lined element. The determination of the dissipation coefficient like also documented by Lahiri et al. [16] is based on a method proposed by Ronneberger [21] and his students [3,8].
For each configuration two different sound fields are excited consecutively in two separate measurements (index a and b). Speaker A (upstream) is used in the first measurement and in the second measurement the same signal is fed into speaker B (downstream). Then, the data of section 1 and section 2 (index 1 and 2) are analyzed separately. This results in four equations for the complex sound pressure amplitudes for each section and measurement:

$$p_{1a}(x) = p_{1a}^{+} e^{-ik_1^{+}x} + p_{1a}^{-} e^{ik_1^{-}x} \tag{1}$$

$$p_{2a}(x) = p_{2a}^{+} e^{-ik_2^{+}x} + p_{2a}^{-} e^{ik_2^{-}x} \tag{2}$$

$$p_{1b}(x) = p_{1b}^{+} e^{-ik_1^{+}x} + p_{1b}^{-} e^{ik_1^{-}x} \tag{3}$$

$$p_{2b}(x) = p_{2b}^{+} e^{-ik_2^{+}x} + p_{2b}^{-} e^{ik_2^{-}x} \tag{4}$$

p^{+} and p^{-} are the complex amplitudes of the downstream and upstream traveling waves with their respective wave numbers $k^{\pm}$. The amplitude of the incident sound wave was set to approx. 110 dB, respectively.
The recorded microphone signals are transformed into the frequency domain using the method presented by Chung[5]. This method rejects uncorrelated noise, e.g. turbulent flow noise, from the coherent sound pressure signals. Therefore, the sound pressure spectrum of one microphone is determined by calculating the cross-spectral densities between three signals, where one signal serves as a phase reference. In our case the phase reference signal is the source signal of the active loudspeaker. As a result we obtain a phase-correlated complex sound pressure spectrum for each microphone signal.
According to Eqs. 1-4 the measured acoustic signal is a superposition of two plane waves traveling in opposite direction. In order to determine the downstream and upstream propagating portions of the wave in each section, Eqs. 1-4 are fitted to the microphone data. As a result of this least-mean-square fit, the four complex sound pressure amplitudes p_1^{+}, p_1^{-}, p_2^{+} and p_2^{-} are identified for both measurements. These sound pressure amplitudes are related to each other via the reflection and transmission coefficients of the test object. This is illustrated in Fig. 3 for the two different measurements A and B. The results from both measurements are combined in order to calculate the reflection and transmission coefficients:

$$r^{+} = \frac{p_{1a}^{-} p_{2b}^{-} - p_{1b}^{-} p_{2a}^{-}}{p_{1a}^{+} p_{2b}^{-} - p_{1b}^{+} p_{2a}^{-}} \qquad r^{-} = \frac{p_{2b}^{+} p_{1a}^{+} - p_{2a}^{+} p_{1b}^{+}}{p_{1a}^{+} p_{2b}^{-} - p_{1b}^{+} p_{2a}^{-}} \tag{5}$$

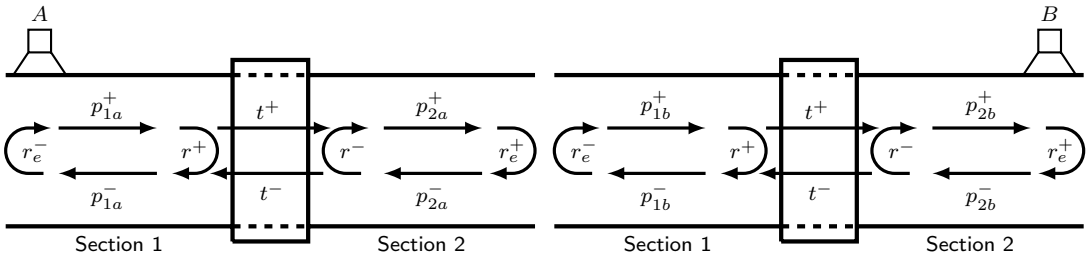

(a) Measurement A, upstream excitation (b) Measurement B, upstream excitation

Fig. 3 Illustration of the sound field in the duct for measurements A and B by means of the sound pressure amplitudes p, the reflection coefficient r, the transmission coefficient t, and the end reflection r_e

$$t^+ = \frac{p_{2a}^+ p_{2b}^- - p_{2b}^+ p_{2a}^-}{p_{1a}^+ p_{2b}^- - p_{1b}^+ p_{2a}^-} \qquad t^- = \frac{p_{1a}^+ p_{1b}^- - p_{1b}^+ p_{1a}^-}{p_{1a}^+ p_{2b}^- - p_{1b}^+ p_{2a}^-} \tag{6}$$

The advantage of combining the two measurements is that the resulting coefficients are independent from the reflection of sound at the duct terminations. These end-reflections are contained in the sound pressure amplitudes, but do not need to be calculated explicitly.

The analysis is applied only in the plane-wave regime (here up to 2100Hz) i.e. the acoustic pressure is constant across the duct cross-section. The frequency range above the cut-on frequency (yielding higher order modes) has been excluded for the reported tests. Thus, the propagating sound wave has always a grazing incidence above the lined surface.

The dissipation of acoustic energy is expressed by the dissipation coefficient. The dissipation coefficient can be calculated from the reflection and transmission coefficients via an energy balance:

$$R^\pm + T^\pm + \Delta^\pm = 1 \tag{7}$$

The energy of the incident wave is partly reflected, partly transmitted, and partly absorbed by the damping module. R and T are the power quantities of the reflection and transmission coefficients, while r and t have been the pressure quantities. Blokhintsev [2] defines the acoustic energy flux I in a moving medium (see as well in [17]):

$$I = \frac{1}{\rho c} \left(1 + M\right)^2 \left\langle p^2 \right\rangle \tag{8}$$

where $\langle p \rangle$ is the time-averaged acoustic pressure, ρ is the density of the medium, c is the speed of sound, and M is the mean Mach number. Integrating over the duct cross-section area A and using the pressure amplitude yields a relation between the acoustic pressure p and acoustic power P quantities:

$$P^\pm = \frac{A}{2\rho c} \left(1 \pm M\right)^2 \left|p^\pm\right|^2 \tag{9}$$

Applying Eq. 9 to R and T in Eq. 7 and then solving for Δ with $A_1 = A_2$, $\rho_1 = \rho_2$, $c_1 = c_2$, and $M_1 = M_2 = M$ yields the definition of the energy dissipation coefficient:

$$\Delta^\pm = 1 - \left(\frac{(1 \mp M)^2}{(1 \pm M)^2} \cdot \left|r^\pm\right|^2 + \left|t^\pm\right|^2 \right) \tag{10}$$

This is an integral value of the acoustic energy that is absorbed while a sound wave is passing the damping module. For further flow case comparisons within this paper the arithmetic average of dissipation coefficients for up- and downstream direction is used.

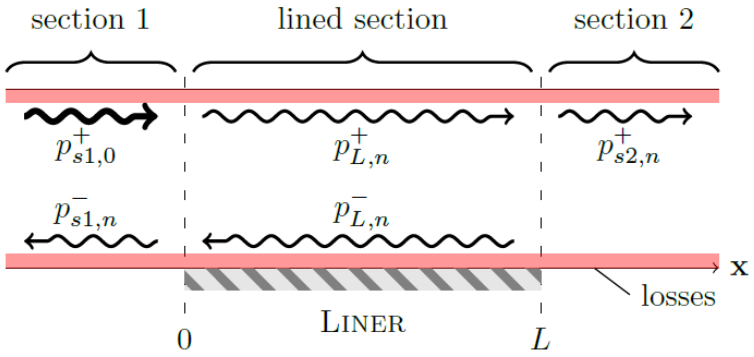

Fig. 4 Sketch of the impedance eduction techniques model D: the incident plane wave enters ($p^+_{1a,b}$ in Fig. 3) from the left hard walled duct section (index: s1), is scattered into the lined section (index: L) and finally into the right hard walled section (index: s2). The model D is two-dimensional: The wave amplitude index '0' refers to plane-wave propagation, 'n' refers to higher-order mode propagation. (from Schulz et al. [22])

In order to evaluate the liner impedance from the scattering coefficients (reflection r and transmission t) the impedance is educed using the model D described in detail in Schulz et al. [22] and sketched in Fig. 4. This impedance eduction model considers the following effects that may influence the propagation of a plane wave through the lined section:

1. Reflections that occur at the two discontinuities of the wall impedance at the leading and the rear end of the lined duct section. So at least two waves traveling in $+x$- and $-x$-direction contribute to the sound field within the lined duct section. This information is extracted from the reflection and transmission coefficients r and t (see also Fig. 3).
2. Higher-order modes are generated at the discontinuities of the impedance. Hence, more than one mode can contribute to the transmission through the lined duct.
3. The structure of the modes differs between the hard-walled and the lined duct. Therefore, near fields at the interfaces between the lined and the hard-walled ducts have to provide for a smooth transition between the plane fundamental modes in the hard-walled duct and the propagable field in the lined duct. The near field which is composed of non-propagable modes, may effect a pressure difference between the propagable fields on either side of the impedance discontinuity.
4. Viscose and thermal losses (marked in red in fig. 4) modify the sound field within a thin acoustic boundary layer at the walls of the duct (in both the hard wall and the lined sections). This may have a sensible effect on the educed impedance.

The method applies an iterative solution via mode matching across the interfaces at the liner leading and trailing edge in order to determine the effective impedance of the liner surface.

2 Hybrid Zero Massflow Liner

The hybrid Zero Massflow Liner (hybrid ZML) concept embraces a combination of a classical Single-Degree-of-Freedom (SDOF) liner and a Zero-Massflow-liner (ZML) design. The SDOF liner principle allows a potentially high damping performance in a rather narrow frequency range (see e.g. [13,18,20,22,4,9]). A ZML liner consists of a perforated face sheet and a cavity below which is excited e.g. by a loudspeaker. It provides a rather broadband damping behavior presumably by the interaction of the periodically oscillating jets through the face sheet perforation with the

acoustic field to be damped (see also [15,14]). It is assumed that acoustic energy is transferred to the production of additional vorticity in the jet shear layer. This damping behavior seems to be comparable to the damping performance of (steady) bias flow liner (see e.g [16]) commonly found in hot stream areas like combustion chambers. However, the ZML concept demands less air / energy (depending on the excitation mechanism) compared to a steady bias flow liner. Earlier investigations by Lahiri et al. [14] demonstrated with the application of the ZML concept an air mass flow reduction of up to 60% compared to a conventional (steady) bias flow liner while providing the same damping performance. However, no optimization was conducted in these investigations.

The principle of the combination of an SDOF and a ZML liner is sketched in figure 5.

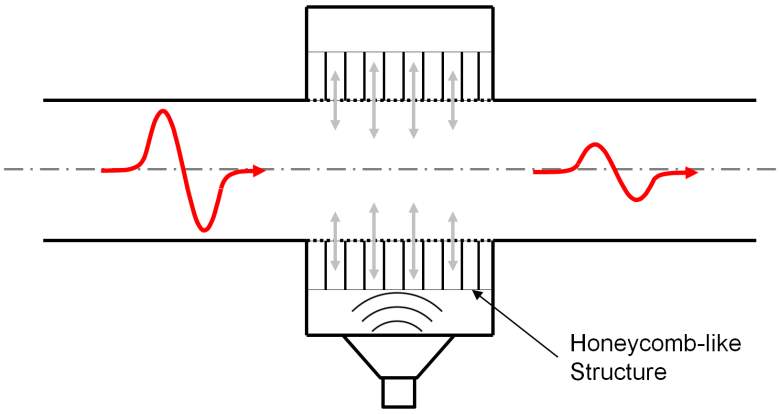

Fig. 5 Sketch of the investigated hybrid ZML-concept combining a conventional honeycomb structure with an excited ZML cavity.

In contrast to conventional active noise control (ANC) systems the ZML damping effect does not need to have a distinct frequency and phase relation between the oscillating flow through the liner perforation and the acoustic sound field (to be damped) in the main duct. This enables the use of liner configurations without closed-loop control algorithms.

The following section presents the damping potential of different realizations of hybrid ZML concepts investigated experimentally in the liner test facility (DLR-DUCT-R) by variation of different parameters like flow conditions, actuation amplitude, and actuation frequency. The design of the ZML samples investigated in the current paper was derived from previous reference liner samples (SDOF) and some experience with the acoustic behavior of liner perforations with bias flow.

2.1 Liner Configurations

The investigated liner samples cover three different types of configurations:

1. The classical Single-Degree-Of-Freedom (SDOF) liner consisting of a perforated face sheet where each perforation hole is connected to one cavity from a honeycomb structure. The honeycomb cells are cylindrical with an inner diameter of 6.9 mm and closed at the backside with a solid back-plate (see also left sketch in figure 6). These samples are called SDOF1 and SDOF2.

Short name	Depth of honeycomb structure (in mm)	Total cavity depth (in mm)	Perforation hole diameter (in mm)	Face sheet porosity (in %)
SDOF1	39 (no add. cav.)	39	1	1.77
SDOF2	39 (no add. cav.)	39	1.5	3.98
hybZML1	30	60	1	1.77
hybZML2	39	60	1.5	3.98
hybZML3	30	60	1.5	3.98
ZML1	-	60	1.5	3.98

Table 1 Overview over liner test samples and specifications

2. A pure ZML setup, where the perforated face sheet is connected to one big single volume which can be acoustically excited by a loudspeaker mounted to the cavity (see also center sketch in figure 6). This sample is called ZML1.
3. Finally the hybrid ZML liner which are a combination of the previous setups. They have the same liner cavity total volume as the pure ZML liner but there is also a honeycomb structure mounted onto the perforated face sheet. But different to the SDOF liner the backside of this honeycomb structure is now open to the remaining total liner cavity (see also right sketch in figure 6). These liner samples are called hybZML1, hybZML2 and hybZML3.

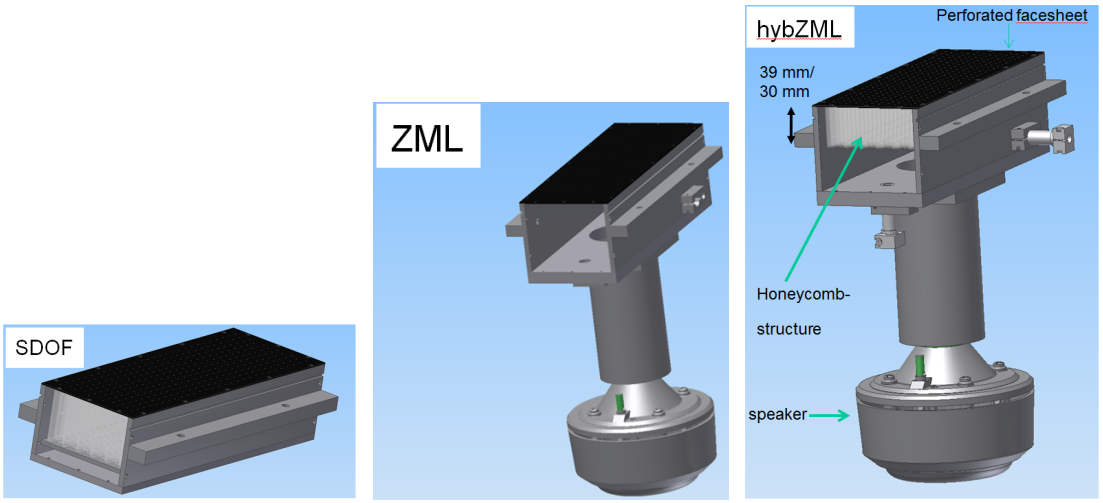

Fig. 6 Schematic view of the three different liner sample types. Left: SDOF; center: ZML; right: hybrid ZML.

For each sample type with respect to the geometrical cavity configuration two different face sheet porosities (1.77 % and 3.98 %) were investigated. This was realized by two different perforation hole diameters of 1 mm and 1.5 mm, respectively. An overview over all liner samples within this study is given in table 1.

2.2 Results

Preceding investigations revealed for all the hybrid liner samples that a liner cavity excitation frequency of about 1000 Hz provides a sufficient high pressure oscillation within the cavity volume in order to drive the pulsating jets through the perforation of the liner face sheet. This cavity

excitation frequency was applied for the ZML (ZML1) and the hybrid ZML liner (hybZML1, hybZML2 and hybZML3) configurations.

2.2.1 Variation of hybrid ZML Excitation Level

In a next step the excitation amplitude was varied by changing the amplitude of the loudspeaker input signal. Therewith, the sound pressure level inside the cavity (measured with one of the cavity microphones as a reference) could be set between 133 dB and 145 dB (corresponding to 100 mV to 700 mV loudspeaker input signal).

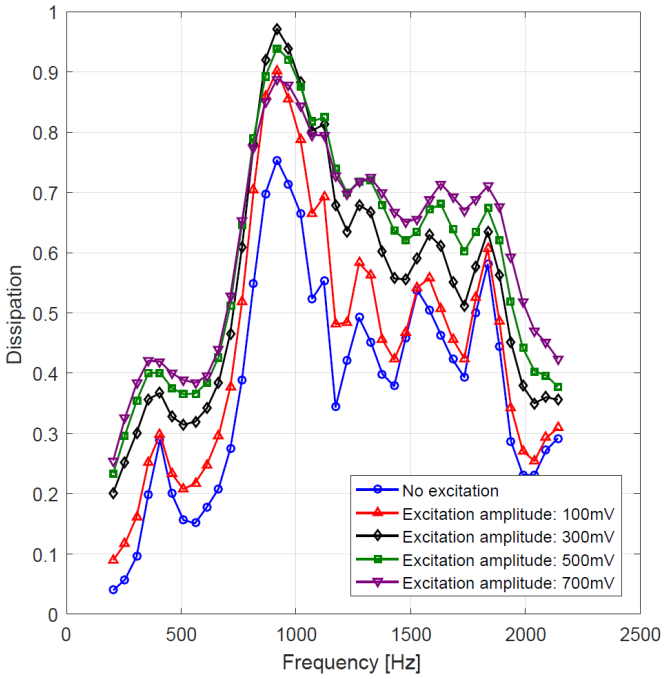

Fig. 7 Dissipation performance (dimensionless) of a hybrid ZML liner (hybZML3) without excitation (blue) and for different excitation amplitudes at 1000 Hz in the liner cavity, without grazing flow.

With the different ZML excitation levels the dissipation (according to Eq. 10) in the duct was determined. As an example figure 7 shows the dissipation behavior for the hybrid ZML sample hybZML3 (30 mm honeycomb depth and $\approx$ 4 % face sheet porosity). Without cavity excitation (blue line) the dissipation characteristics reveal several damping maxima presumably caused by different cavity resonances of the cavity system. The major peak frequencies (408 Hz, 918 Hz, and 1836 Hz) have quarter wavelength of about 210 mm, 93 mm, and 47 mm (with a speed of sound of 343 m/s). These values do not easily fit to any geometric dimensions of the liner sample. Therewith, is it difficult to provide a simple geometric explanation or even a prediction of these peak frequencies. An increase of the cavity excitation improves the dissipation both at the main damping maximum at around 900 Hz as well as in a broadband range at lower (200-700 Hz) and at higher (1000-2000 Hz) frequencies. The main damping maximum reaches an optimum with a dissipation of almost 1 at a loudspeaker input signal of 300 mV (black line) which corresponds to a cavity sound pressure level of $\approx$ 140 dB. A further increase of the cavity excitation amplitude

enhances the broadband dissipation with some reduction at the main damping maximum (see green and violet line).

2.2.2 Resistance Effect vs. additional ZML Damping

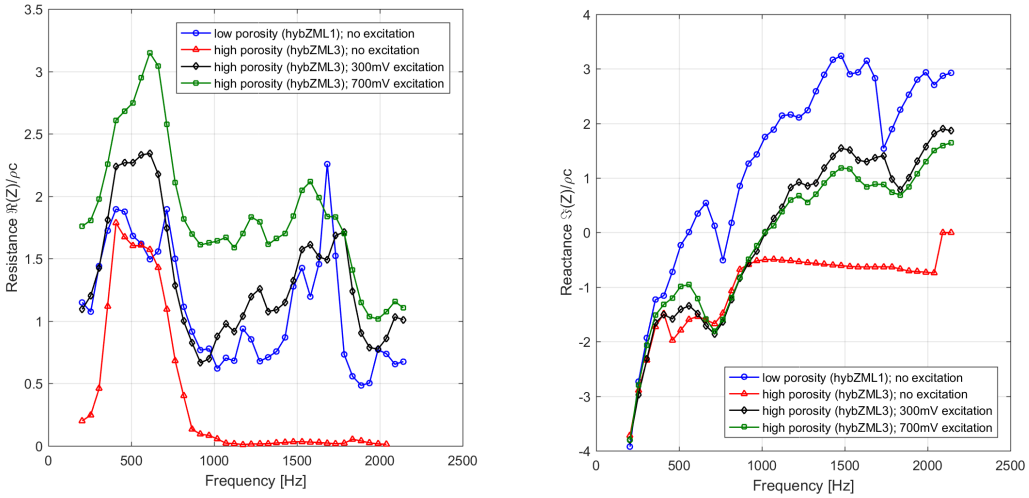

Fig. 8 Comparison of the educed complex impedance (see section1.2) of a (non-excited) hybrid ZML liner (hybZML1) with a higher face sheet resistance (lower porosity) to an excited hybrid ZML liner (hybZML3) with a lower face sheet resistance (higher porosity) without grazing flow (in addition the non-excited hybrid ZML liner (hybZML3) with a lower face sheet resistance (higher porosity) is included). Left: Resistance; right: Reactance

One main question arising from this observation is whether the increase of dissipation with the cavity excitation is only caused by the increased face sheet resistance. In principle the face sheet resistance of a liner can increase with

- the reduction of the face sheet porosity
- an increasing grazing mean flow Mach number
- an increase of steady bias flow through the perforation
- an increasing periodic bias through the perforation (like in case of the ZML excitation)

This means that changing the ZML excitation amplitude also 'produces' a resistance variation. For each liner-duct-setup it exists an 'optimal' resistance where the dissipation peak reaches a maximum. Theoretically the best guess here for the optimal impedance follows the approach of Cremer [6] further developed by Tester [24]: $Z_{opt}/(\rho * c) = ((2 * h)/\lambda) * (0.929 - i * 0.744)$. For the duct dimension $h = 60$ mm and a frequency of 820 Hz under atmospheric conditions this yields an optimal normalized impedance of $Z_{opt}/(\rho * c) \approx 0.29 - i * 0.21$. Here, the resistance seems to reach the 'optimal' value with respect to the liner-duct setup for the frequency range around 900Hz at an excitation amplitude of 300 mV (black line in figure 7). However, this would

In order to evaluate the resistance effect of the ZML excitation the impedance has been educed for the cases without grazing flow according to the impedance eduction procedure outlined in section 1.2. Figure 8 shows on the left-hand side the real part of the impedance (resistance) and on the right side the imaginary part (reactance) of a non-excited liner with a high face sheet

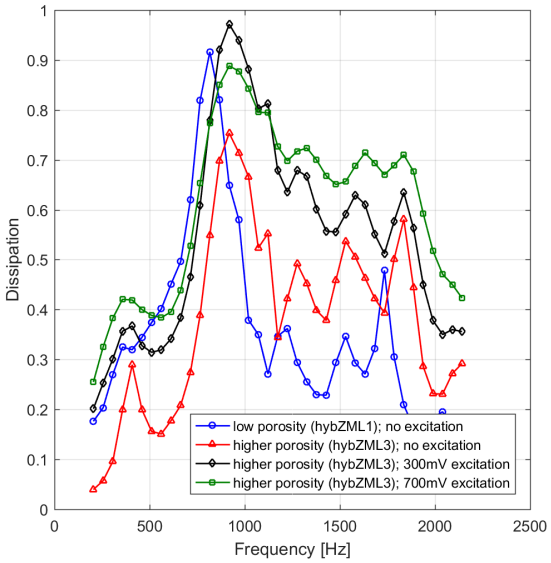

Fig. 9 Comparison of the dissipation performance (dimensionless) of a (non-excited) hybrid ZML liner (hybZML1) with a higher face sheet resistance (lower porosity) to a non-excited and excited hybrid ZML liner (hybZML3) with a lower face sheet resistance (higher porosity) without grazing flow.

resistance (= low face sheet porosity: 1.77 %; hybZML1) compared to an excited liner with a lower face sheet resistance (here hybZML3; higher face sheet porosity: 3.98 %). It is obvious that the resistance of the non-excited, low face sheet porosity liner (hybZML1) is comparable to the excited, high face sheet porosity liner (hybZML3; 300 mV) over a broad frequency range. A higher ZML excitation amplitude (hybZML3; 700 mV) reveals a further increase of the resistance values. The non-excited high face sheet porosity liner (hybZML3; not shown here for better readability) provides a significant lower resistance than hybZML1 / hybZML3-300 mV. The discrepancy of the resistance values educed from the acoustic measurements to the theoretical optimal impedance given by Tester [24] is not fully clear yet. It is assumed that the low aspect ratio of the duct (60mm by 80mm) compared to the two-dimensional theory may be one of the reasons for this deviation. The reactance values (right side of figure 8) show a fairly similar liner-specific behavior where the ZML excitation amplitude has no major influence.

To separate the pure resistance effect from a potential, additional ZML effect, Figure 9 shows the corresponding dissipation coefficients. It can be observed that the values of the damping maximum at around 800 Hz are comparable between the non-excited (low porosity, hybZML1) liner (blue line) and the excited (high porosity, hybZML3) liner (black line: excitation amplitude = 300 mV). However, the excited liner case indicate a significant additional increase of broadband dissipation up to 0.7 in a frequency range between 1200 and almost 2000 Hz (see excited cases (black line) in figure 9). Since the resistance is comparable like shown in figure 8 the only difference between the two configurations is an additional damping effect due to the interaction of the externally forced, periodic pulsation jets through the liner face sheet with the acoustic field propagating in the duct. This observation suggest that the impedance itself, which is very similar between the excited (high porosity, hybZML3) liner and the non-excited (low porosity, hybZML1) liner, is not sufficient to describe the acoustic damping characteristics of a hybrid

ZML configuration. This reveals the need for an additional describing parameter for the acoustic behavior of a hybrid ZML system.

2.2.3 Comparison of SDOF - ZML - hybrid ZML liners

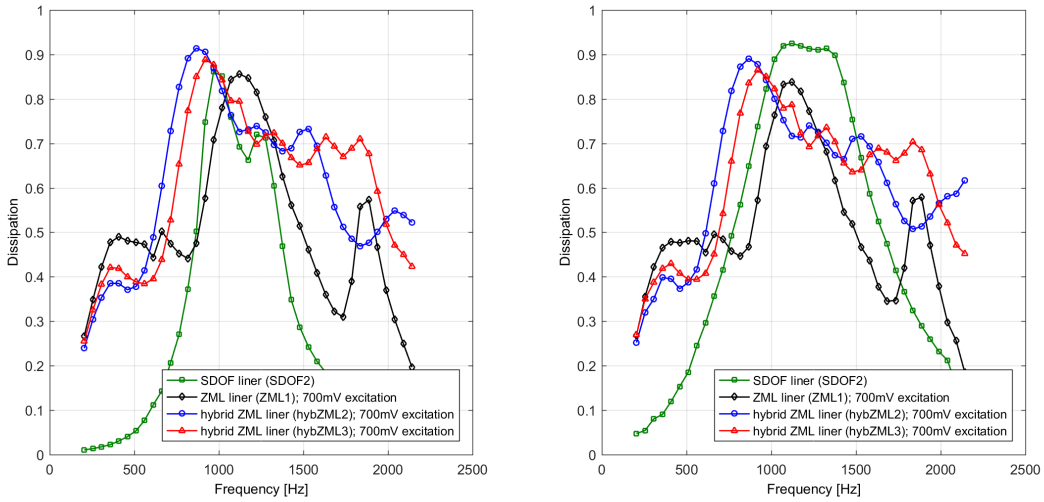

Fig. 10 Comparison of the dissipation performance (dimensionless) of an SDOF liner (SDOF2), an excited 'pure' ZML liner (ZML1) and two excited hybrid ZML liner (hybZML2 and hybZML3). Left: Without grazing flow; right: With grazing flow Mach number of 0.1.

One of the objectives of these investigations was the evaluation of the damping performance of the three types of liner concepts. Figure 10 shows the corresponding dissipation coefficients of an SDOF liner (SDOF2), an excited 'pure' ZML liner (ZML1) and two excited hybrid ZML liners (hybZML2 and hybZML3) without grazing flow (left) and with a grazing flow Mach number of 0.1 (right). The SDOF liner (SDOF2) provides as expected a relevant dissipation value only in a fairly narrow frequency range (800 Hz to 1500 Hz). Outside of this frequency range the SDOF exhibits a dissipation below 30 %. In comparison the 'pure' ZML excited liner (ZML1; 700 mV) shows an increase of dissipation in the low frequency range (300 Hz to 800 Hz) to almost 50 % dissipation. In addition this liner reveals another dissipation peak of about 55 % in the vicinity of 1800 Hz. The two excited, hybrid ZML liners (hybZML2 and hybZML3; 700 mV) have a shifted dissipation maximum to a lower frequency of about 800 Hz and 900 Hz, respectively. Both liners also provide increased low frequency dissipation of 40 % in the range between 300 Hz and 700 Hz. At frequencies above the dissipation maximum both hybrid ZML liners show a significant high level dissipation value of about 70 % for a very broad frequency range. In case of the hybZML3 this high dissipation ranges to frequencies up to almost 2000 Hz. This emphasizes the increased damping potential of the hybrid ZML liner concept.

2.2.4 Influence of Grazing Flow

The next part of the parametric study addressed the influence of grazing flow on the identified ZML damping effect.

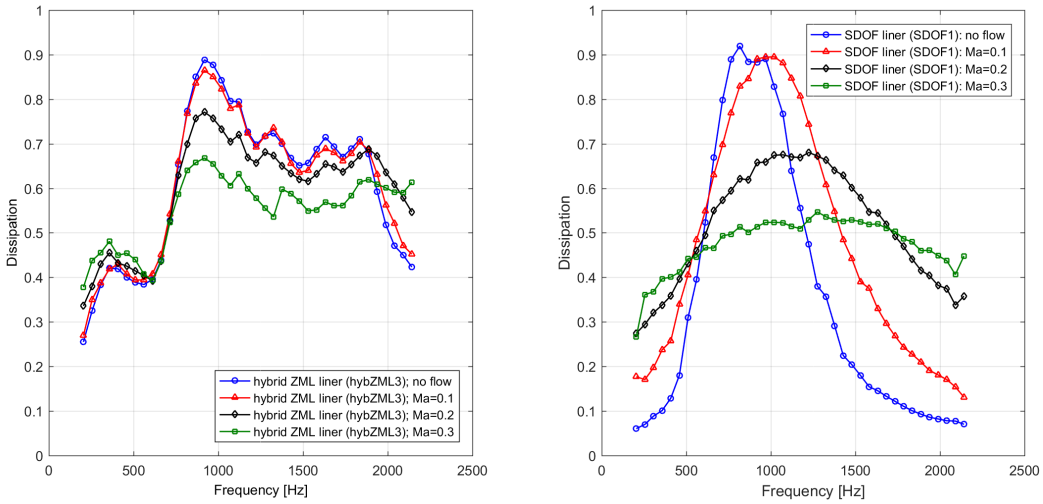

Fig. 11 Dissipation performance (dimensionless) of a hybrid ZML liner (hybZML3; left) with constant liner cavity excitation (1000 Hz, 700 mV) and of a conventional SDOF liner (SDOF1; right) for different grazing flow Mach numbers.

Figure 11 displays in the left graph the dissipation coefficients of the hybrid ZML liner hybZML3 for different grazing flow Mach numbers (0 to 0.3) with a cavity excitation of 700 mV at 1000 Hz. The increasing grazing flow Mach number reduces the maximum dissipation peak value around 800 Hz while enhancing slightly the dissipation at lower ($\leq$ 500Hz) and at higher ($\geq$ 1700Hz) frequencies. A variation of the liner cavity excitation amplitude (not shown here) reveals that the impact of the ZML excitation vanishes with higher grazing flow Mach numbers (here limited by the maximum duct Mach number of the test rig at 0.3). This is probably caused by the strong increase of the face sheet resistance with the grazing flow (see above) which seems to fully override any potential ZML excitation benefit. In order to confirm this hypothesis it would be necessary to design ZML liner samples with even higher face sheet porosity in order to obtain the 'optimal' resistance under grazing flow conditions. Then the additional ZML damping effect might be noticeable. On the right graph of figure 11 the typical dissipation behavior of a conventional SDOF liner (here SDOF1) under different grazing flow conditions is displayed. Increasing the grazing flow Mach number reduces here also the damping maximum while broadening the dissipation performance to an extended frequency range.

3 FlexiS-Liner

The second liner concept for an enhanced acoustic damping performance relies on the interaction of the sound field with flexible walls within the liner cavity structure. Hereby, the deflection of the cell walls and intrinsic damping of the wall material shall lead to an improved damping characteristics in terms of overall absorption (dissipation) of acoustic energy and shall enlarge the frequency range of significant absorption.

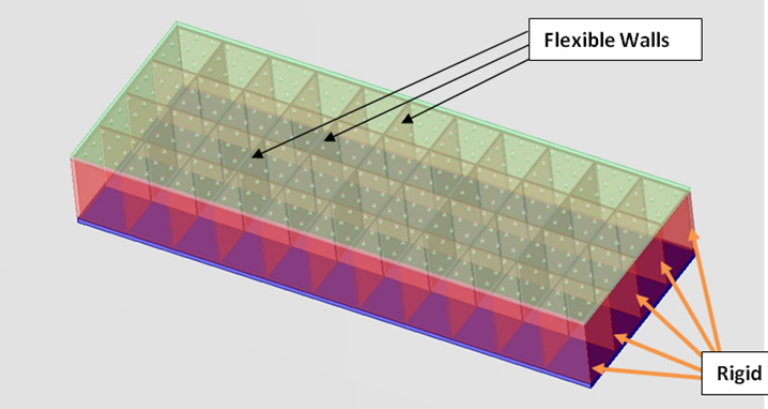

Fig. 12 Principle setup of FlexiS liner concept with partially flexible walls in the liner cavity structure.

3.1 Liner Configurations

The basic setup of the liner samples investigated in the framework of this study is comparable to a conventional Helmholtz-Resonator liner (SDOF). The samples consist of four by ten liner cavities in span-wise and flow direction, respectively. These cavities are 19 mm by 19 mm in width and length and 30 mm in depth. As an interface to the acoustic duct the cavities are covered with perforated face-sheet. The perforation is setup in a way that each cavity is provided with nine holes of 1.3 mm diameter. The overall cell and perforation geometry were selected in order to establish a damping maximum around 1000 Hz, which allows a detailed investigation of all samples - with and without grazing flow - in the plane-wave regime of the duct facility.

A reference configuration with completely rigid walls serves as the baseline case for the comparison of the damping performance. In the new liner concept (FlexiS) the walls perpendicular to the sound field propagation direction are designed with flexible material like shown in figure 12. The material for the flexible walls was selected due to their inherent damping properties. Usually, this property is determined by a DMA (dynamic mechanical analysis), which measures the phase difference between stress and strain. The tangent of this phase difference is the loss factor characterizing the inherent damping. For the wall material it is not known a priori, whether a high loss factor $\tan(\delta)\geq 1$ should be preferred in comparison with an intermediate value of $\tan(\delta)\approx 0.3\text{-}0.5$. However, since the loss factor depends on frequency (i.e. speed of deformation) and temperature, a material with a small variation of loss factor over frequency is preferred for the experiments. The choice of materials therefore included commercially available Thermoplastic-polyurethan materials (TPU), which exhibit an intermediate loss factor and are available in various types and thicknesses ranging from one tenth of a millimeter to several millimeters. Material parameters can be obtained from material data sheets (e.g. from BASF [1]) or determined as described above. A second material with a high loss factor was custom made by a project partner from epoxy resin in combination with polyetheramine in a thickness of 0.5 mm. It is denoted as as “EP-0.5”. Overall, three different flexible composite materials in different thicknesses between 0.1 and 0.5 mm (1170-0.3, 1195-0.1, 1195-0.5, EP-0.5) were investigated during this study.

During the design process of the experiment and the liner, it was considered that the deflection of the flexible walls is the most important element for the anticipated effect. However, the magnitude of the deflection could not be guessed with sufficient accuracy or determined with preliminary experiments due to the unknown boundary and excitation conditions of the flexible walls inside the actual liner. Therefore it was decided to set up a liner model, which could be

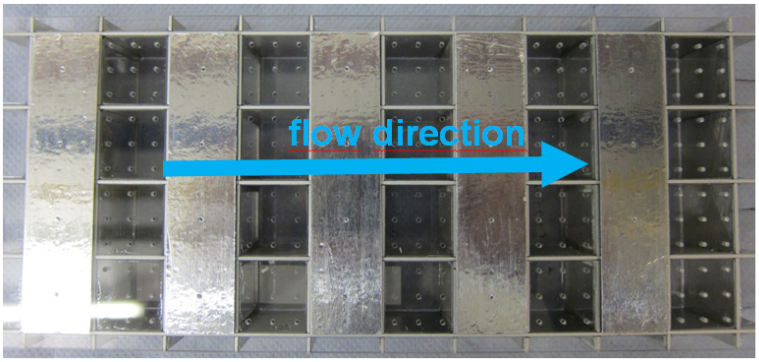

Fig. 13 Photo of FlexiS liner in the partially taped configuration in order to enhance the wall deflection between active (non-taped) and inactive (taped) cells.

used for a large set of experiments and allows for adaptations e.g. by taping certain sections with a rigid aluminum tape. A second advantage of this configuration is the ease of the manufacturing process using a rectangular slit connection system.

In the series of experiments presented first, a certain part of the cells have been covered with tape in order to enhance the inter-cell wall deflection. Therewith, the tape covered cells behave acoustically inactive meaning they are not directly impacted by the grazing sound field in the duct. In this case a fluctuating pressure difference on both sides of the flexible cell walls is generated – forcing the wall to an increased movement. In the chosen setup every second spanwise cell row like shown on the photo in figure 13 was taped and only ventilated by a pinhole in order to compensate pressure differences in the system during operation of the flow duct. Since these ventilation pinholes are fairly small, it was assumed that they do not alter the acoustic damping characteristics of the overall liner significantly in the frequency range of interest for this study.

3.2 Experimental Results

The acoustic characterization with respect to the dissipation coefficients has been determined again in the DUCT-R liner test facility at DLR Berlin as described in sections 1.1 and 1.2.

Figure 14 shows for the taped configurations like shown on the photo in figure 13 the comparison of the dissipation coefficients in the no flow case. Here, also the reference Helmholtz-Resonator liner with rigid walls was taped the same way in order to compare the same active area for all liner samples. Most of the applied flexible materials demonstrate a significant increase for the dissipation in the low frequency range from 400 to 800 Hz. While the EP-0.5 material generates a broadening of the dissipation peak, the material 1170-0.3 shows even three dissipation maxima at 600, 1000 and 1350 Hz. The three dissipation maxima were not expected a priori. It was assumed that the flexible walls may act in different ways on the overall dissipation of the liner. Key point is certainly the deflection of the wall requiring additional energy which originates from the acoustic field inside the cavity. If several eigenmodes/eigenfrequencies are excited (these strongly depend on the material of the wall and the boundary conditions), then, more than one local maximum might occur. This could be the case for the observed damping behaviour of the liner with 1170-0.3 walls. However, a detailed in-situ investigation of the movement of the flexible walls would be required in order to verify the supposed mechanism.

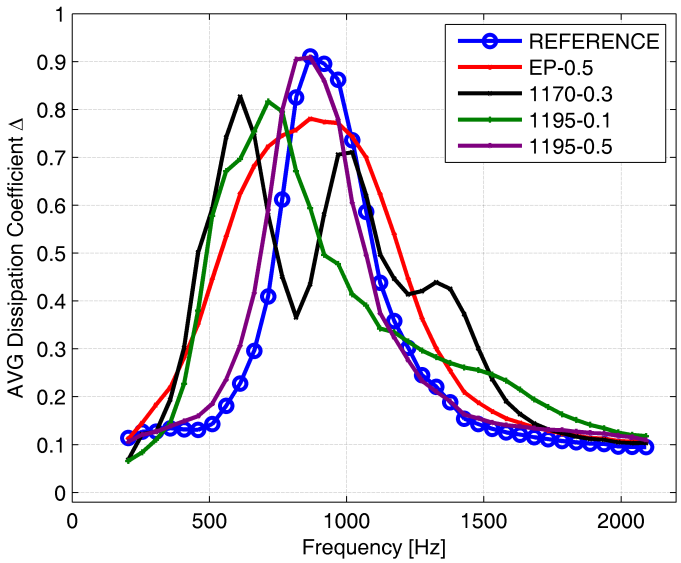

Fig. 14 Dissipation coefficient (dimensionless) of several FlexiS liner with different flexible wall material in the taped configuration compared to the (also taped) reference Helmholtz-Resonator liner (HR) in the no flow case (sound field excitation level: 120dB).

For the sample with the material 1195-0.1 the dissipation maximum is shifted from 900 Hz (REFERENCE) to around 750 Hz.

All FlexiS liner samples show a reduction of the maximum dissipation value. However, the integrated overall dissipation over the entire frequency range is increased. This shows the additional damping mechanism by the deflection of the flexible walls with the intrinsic material damping characteristics.

In the case with grazing flow the observed behavior is comparable to the no flow case as shown in figure 15 for a grazing flow Mach number of 0.2. In general, the grazing flow reduces the total dissipation of the liner samples. But since this affects all liner samples including the reference sample with rigid walls the relative changes in dissipation behavior are similar to the no flow case.

The experiments were performed using multi-tone excitation with an overall sound pressure level (OASPL) of 120 dB and repeated for 130 dB (not shown in this paper). Since the processing of the data yields non-dimensional quantities of reflection, transmission, and dissipation, the results of both series of experiments can be easily compared. It is known from the investigation of classical Helmholtz-resonator liners, that for the no-flow case some non-linearities occur above 120 dB if no grazing flow is present. With grazing flow, the linear behavior (with respect to the amplitude of the grazing sound field) holds beyond the value of 120 dB. The same observations were made for the FlexiS-liner - with dissipation curves for 120 dB and 130 dB being almost identical. It is assumed, that the excitation of the flexible wall structure occurs near the resonance frequency of the cavity, where the sound pressure level inside the cell will be higher than the SPL of the grazing sound field due to the (damped) resonance. More detailed investigations of the movement of the flexible walls (local deflection, eigenforms) is required in order to understand the mechanisms acting inside the cavities.

In order to validate the additional damping mechanism and to prove the geometric conformity of all FlexiS liners with the reference Helmholtz-Resonator liner the liner samples have been

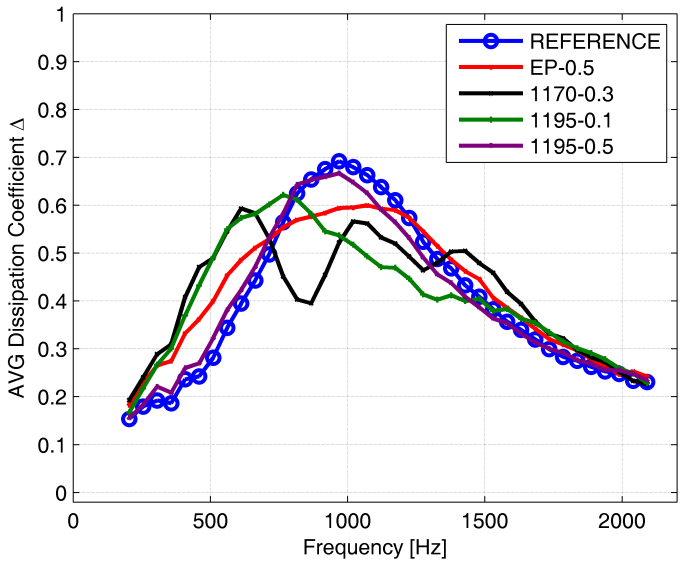

Fig. 15 Dissipation coefficient (dimensionless) of several FlexiS liner with different flexible wall material in the taped configuration compared to the (also taped) reference Helmholtz-Resonator liner (HR) with a grazing flow Mach number of 0.2 (sound field excitation level: 120dB).

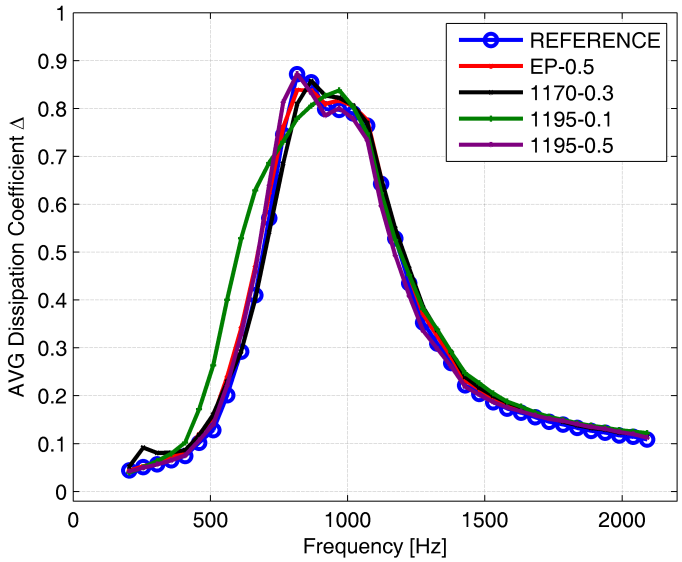

Fig. 16 Dissipation coefficient (dimensionless) of several FlexiS liner with different flexible wall material compared to the reference Helmholtz-Resonator liner (HR) in the no flow case (sound field excitation level: 120dB).

tested in the non-taped configuration in another series of this investigation. Hereby, as shown in figure 16 for the no flow case, the dissipation behavior of the FlexiS liner samples (EP-0.5, 1170-0.3, 1195-0.1, 1195-0.5) with flexible walls differs only slightly from the reference Helmholtz-Resonator sample with rigid walls (REFERENCE). All liner samples indicate the same maximum dissipation for frequencies around 800 to 1000 Hz. Only one flexible wall material (1195) with a thickness of 0.1 mm (green line) exhibits some dissipation increase compared to the reference sample in a frequency range between 400 and 700 Hz.

This agreement of dissipation characteristics, which also applies for the grazing flow cases but is not shown here, confirms that the phase difference between two in propagation direction subsequent cells is too small for an sufficient oscillation excitation of the flexible walls in between. For this reason no additional acoustic damping is achieved and the FlexiS liner samples behave like conventional Helmholtz-Resonator liner.

Influence of Pinholes

Further experiments were made in order to verify, that the improved acoustic damping performance is not only the result of additional resonator cells with lower resonance frequency. For each cavity which was covered by the tape, the pinhole was made in the middle hole of the perforation. The diameter of the pinholes are not well defined, but in the range between 0.5 and 1 mm. Latter value yields an estimate for the Helmholtz resonance frequency of 280 Hz. For these experiments, starting from the "TAPED" configuration of the reference liner, the remaining open cells were also covered by the aluminium tape, but without pinholes. Thereby, the observed damping should be solely caused by the pinholes and some marginal effect of the aluminium tape which is not as stiff as a rigid wall.

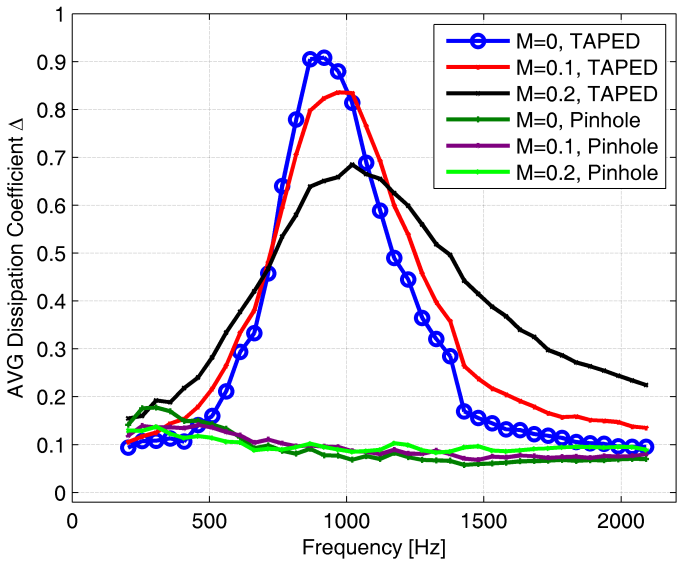

Fig. 17 Dissipation coefficient (dimensionless) of the reference Helmholtz-Resonator liner in "TAPED" configuration and the effect of pinholes for M=0–0.2(sound field excitation level: 130dB).

These results in figure 17 confirm, that the observed effects in the broadening of the acoustic dissipation peaks (figure 14) is not directly owed to the presence of an additional resonator with low frequency resonance.

The results presented for the FlexiS liner reveal the enhanced damping potential of this liner concept with flexible wall structures and additional material damping. This concept allows to broaden the effectively damped frequency range and to shift the damping characteristics to lower frequencies without increasing the liner size and without the demand of additional energy.

In the current investigation, the arrangement of active (open) and non-active (taped) cells allowed for a great flexibility in liner setup without comprehensive changes or re-manufacturing of the liner. However, in terms of an efficient damping of acoustic energy, this setup represents a loss in active damping surface. Therefore, future works needs to address the influence and requirements for the non-active parts (required size, coupling between neighboring non-active cavities, best placement, etc.) in order to find an optimal arrangement.

4 Summary and Conclusions

This article presents two different novel concepts for advanced liner with enhanced broadband acoustic damping performance.

The application of hybrid ZML liner samples can improve the broadband absorption by acoustically exciting the liner cavity. Various configurations of SDOF, ZML and hybrid ZML liner configurations have been investigated. To keep the paper reasonable in length only part of the results have been exemplarily presented. In order to discriminate the dissipation benefit from the effect of a pure resistance increment, samples with different levels of face sheet porosity have been compared. This enabled the separation of 'pure resistance' effect from 'ZML related' effects on the damping performance. The latter one impacts mainly a significant increased broadband damping in a frequency range between 1200 and 2000Hz. These results lead to the conclusion that for the description of the acoustic characteristics of hybrid ZML liners an additional parameter besides the impedance needs to be derived and determined. The current study shows that grazing flow reduces the ZML benefit for this set of hybrid liner samples. This is presumably caused by the strong flow induced increment of the face sheet resistance. It is expected that a face sheet design accounting for even lower resistance values at no-flow conditions would overcome this implication and would provide increased dissipation values under grazing flow conditions. For a real scale application of this liner concept, e.g. in aero-engines, loudspeakers as the excitation source for the liner cavity may not be appropriate. Here, an aeroacoustic actuator like a jet-edge configuration (flute principle) driven by bleed air may be integrated. First investigations of this ZML actuator realization with a cavity excitation level of more than 150 dB have been provided by Lahiri et al. [14]. The detailed physical damping mechanism of the additional ZML effect is yet not fully understood. This is still under investigation in ongoing research with one of the objectives to derive a suitable model description for future design and optimization processes.

The second concept being presented here (FlexiS liner) is based upon the acoustic-structure interaction withing the liner cavities. Hereby, part of the inter-cell walls are designed with flexible composite material with additional intrinsic damping properties. These liner concepts provide a significant damping improvement especially at lower frequencies when the deflection of the flexible walls is enhanced. This was realized by keeping part of the liner cells acoustically inactive meaning that these cells have no direct connection to the acoustic duct. Transferring this concept to full scale application these inactive cells could be arranged differently, e.g. between the active cells and the solid back-plate. Compared to DDOF concepts the FlexiS liner may provide additional intrinsic (structure/material based) damping by the oscillating flexible wall segment.

With respect to the application of the FlexiS concept to full scale aero-engines it is expected that the FlexiS liner will still be effective (if not even more effective) at higher mode orders of the incident sound field because it benefits from local phase differences of the grazing sound field above the liner.

Both novel liner concepts demonstrated a high potential for addressing the needs of modern low emission aero-engines in broadband and low frequency damping performance.

Acknowledgements The authors gratefully acknowledge the valuable contributions of Anita Schulz, Albert Bauer and the LAKS consortium as well as the fruitful discussions with Christoph Richter from Rolls-Royce Deutschland LTD & Co KG. The research leading to these results has received funding from the German Federal Ministry for Economic Affairs and Energy (Luftfahrtforschungsprogramm V) within the framework of the LIST ('Das **L**eise **I**n**S**tallierte **T**riebwerk') project under grant agreement no. 20T1307B and within the framework of LAKS ('**L**ärm**a**bsorbierende **K**unststoff**s**trukturen') project under grant agreement no. 20E1502A.

References

1. BASF: Thermoplastic polyurethane elastomeres. URL http://www.polyurethanes.basf.de/pu/solutions/elastollan/de/function/conversions:/publish/content/group/Arbeitsgebiete_und_Produkte/Thermoplastische_Spezialelastomere/Infomaterial/elastollan_material_uk.pdf. Elastollan® - Material Properties, issued September 2017, accessed online at http://www.polyurethanes.basf.de/pu/Elastollan/Elastollan_Materialeigenschaften on 07 November 2017
2. Blokhintsev, D.I.: Acoustics of a nonhomogeneous moving medium. NACA Technical Memorandum 1399 (1956). Originally published 1946 in russian language
3. Brandes, M.: Optimierung eines Meßvervahrens zur Bestimmung von akustischen Parametern im durchströmten Rohr. Diploma thesis, Universität Göttingen (1992)
4. Busse-Gerstengarbe, S., Bake, F., Enghardt, L., Jones, M.G.: Comparative study of impedance eduction methods, part 1: Dlr tests and methodology. In: 19th AIAA/CEAS Aeroacoustics Conference, 2013-2124. Berlin, Germany (2013). Number of citations (Google Scholar 2015): 4
5. Chung, J.Y.: Rejection of flow noise using coherence function method. Journal of the Acoustical Society of America **62**, 388–395 (1977)
6. Cremer, L.: Theorie der luftschall-dmpfung im rechteckkanal mit schluckender wand und das sich dabei ergebende hchste dmpfungsmass. Acoustica **3**(2), 249–263 (1953)
7. Drevon, E.: Measurement methods and devices applied to a380 nacelle double degree-of-freedom acoustic liner development. In: 10th AIAA/CEAS Aeroacoustics Conference, AIAA 2004-2907 (2004)
8. Enghardt, L.: Bestimmung akustischer Streufaktoren im durchströmten Rohr – Optimierung von Mikrofonanordnung und Meprozedur. Diplomarbeit, Universität Göttingen, Göttingen (1992)
9. Fischer, A., Bake, F., Bassetti, A.: The acoustic-particle velocity in the vicinity of a liner: a piv-caa comparison. In: 19th AIAA/CEAS Aeroacoustics Conference, 2013-2055. Berlin, Germany (2013). Number of citations (Google Scholar 2015): 2
10. Jones, M., Nark, D., Watson, W., Howerton, B.: Variable-depth liner evaluation using two nasa flow ducts. In: 23rd AIAA/CEAS Aeroacoustics Conference, 2017-3022. Denver, Colorado, USA (2017). Number of citations (Google Scholar 2015): -
11. Jones, M., Watson, W., Nark, D., Howerton, B.: Evaluation of variable-depth liner configurations for increased broadband noise reduction. In: 21st AIAA/CEAS Aeroacoustics Conference, 2015-2697. Dallas, Texas, USA (2015). Number of citations (Google Scholar 2015): -
12. Jones, M., Watson, W., Nark, D., Schiller, N., Born, J.: Experimental investigation of sound field decomposition with higher order modes in rectangular ducts. In: 22nd AIAA/CEAS Aeroacoustics Conference, 2016-2783. Lyon, France (2016). Number of citations (Google Scholar 2016): -
13. Jones, M.G., Parrott, T.L., Watson, W.R.: Comparison of acoustic impedance eduction techniques for locally-reacting liners. In: 9th AIAA/CEAS Aeroacoustics Conference and Exhibit, AIAA 2003-3306. Hilton Head, South Carolina (2003)
14. Lahiri, C., Pardowitz, B., Bake, F., Enghardt, L.: The application of an aeroacoustic actuator in a zero mass flow liner for acoustic damping. In: 17th AIAA/CEAS Aeroacoustics Conference, 2011-2725. Portland, USA (2011). Number of citations (Google Scholar 2015): -
15. Lahiri, C., Pardowitz, B., Bake, F., Röhle, I., Enghardt, L.: Excitation of a zero mass flow liner for acoustic damping. AIAA Journal **49**(3), 513–519 (2011)
16. Lahiri, C., Sadig, S., Gerendas, M., Enghardt, L., Bake, F.: Establishment of a high quality database for the modelling of perforated liners. Journal of Engineering for Gas Turbines and Power **133**(9), 091,503–1 – 091,503–9 (2011). Number of citations (Google Scholar 2015): 18

17. Morfey, C.L.: Acoustic energy in non-uniform flows. Journal of Sound and Vibration **14**(2), 159–170 (1971)
18. Murray, P.B., Ferrante, P., Scofano, A.: Manufacturing process and boundary layer influences on perforate liner impedance. In: 11th AIAA/CEAS Aeroacoustics Conference (26th AIAA Aeroacoustics Conference), AIAA 2005-2849. Monterey, California (2005)
19. Redmann, D., Pongratz, R., Zillmann, J.: Aeroacoustic liner applications of the broadband special acoustic absorber concept. In: 19th AIAA/CEAS Aeroacoustics Conference, 2013-2176. Berlin, Germany (2013)
20. Rienstra, S., Hirschberg, A.: An Introduction to Acoustics. Eindhoven University of Technology press (2008). Report IWDE 92–06
21. Ronneberger, D.: Genaue Messung der Schalldämpfung und der Phasengeschwindigkeit in durchströmten Rohren im Hinblick auf die Wechselwirkung zwischen Schall und Turbulenz. Habilitation thesis, Universität Göttingen (1975)
22. Schulz, A., Bake, F., Enghardt, L., Ronneberger, D.: Impedance eduction of acoustic liners based on four different levels of physical modeling. In: 22nd AIAA/CEAS Aeroacoustics Conference, 2016-2726. Lyon, France (2016). Number of citations (Google Scholar 2016): -
23. Smith, M.J.T.: Aircraft noise. Cambridge aerospace series. Cambridge University Press (1989)
24. Tester, B.J.: The propagation and attenuation of sound in lined ducts containing uniform or plug flow. Journal of Sound and Vibration **28**(2), 151–203 (1973)
25. Yu, J., Chien, E.: Folding cavity acoustic liner for combustion noise reduction. In: 12th AIAA/CEAS Aeroacoustics Conference (27th AIAA Aeroacoustics Conference), AIAA 2006-2681. Cambridge, USA (2006)